Converting any Faradaic Current Generated at an Electrode under Potentiostatic Control into a Remote Fluorescence Signal

Rabia Djoumer, Agnès Anne, Arnaud Chovin, Christophe Demaille, Corinne Dejous, Hamida Hallil, Jean-Luc Lachaud

HAL Id: hal-02120999

https://hal.science/hal-02120999

Submitted on 6 May 2019

Converting any Faradaic Current Generated at an Electrode under Potentiostatic Control into a Remote Fluorescence Signal

Rabia Djoumer,† Agnès Anne,† Arnaud Chovin,†* Christophe Demaille,†* Corinne Dejous,‡ Hamida Hallil,‡ Jean-Luc Lachaud‡

† Laboratoire d'Electrochimie Moléculaire, UMR 7591 CNRS, Université Paris Diderot, Sorbonne Paris Cité, 15 rue Jean-Antoine de Baïf, F-75205 Paris Cedex 13, France.

‡ Université de Bordeaux, Bordeaux INP, IMS, UMR5218 CNRS, F-33405 Talence, France.

ABSTRACT: We describe the development of an original faradaic current to fluorescence conversion scheme. The proposed instrumental strategy consists in coupling the electrochemical reaction of any species at an electrode under potentiostatic control, with the fluorescence emission of a species produced at the counter electrode. In order to experimentally validate this scheme, the fluorogenic species resazurin is chosen as a fluorescent reporter molecule, and its complex reduction mechanism is first studied in unprecedented details. This kinetic study is carried out by recording simultaneous cyclic voltammograms and voltfluorograms at the same electrode. Numerical simulations are used to account for the experimental current and fluorescence signals, to analyze their degree of correlation, and to decipher their relation to resazurin reduction kinetics. It is then shown that, provided that the reduction of resazurin takes place at a micrometer-sized electrode, the fluorescence emission perfectly tracks the faradaic current. By implementing this ideal configuration at the counter electrode of a potentiostatic setup, it is finally demonstrated that the oxidation reaction of a non-fluorescent species at the working electrode can be quantitatively transduced into simultaneous emission of fluorescence.

The development of nanoelectrochemistry has prompted the need for measuring ever smaller faradaic currents at electrodes. Direct electrochemical measurement of very low currents (e.g. in the fA range), is a delicate instrumental task, requiring cutting-edge electronics, and has thus only been achieved by a hand-full of research groups pioneering electrochemical nanofluidics[1,2] or nano-SECM.[3–6] Achieving an even greater current sensitivity, as may for example be required for characterizing the activity of individual enzyme molecules or artificial nano-catalysts with slow turnovers, may simply be impossible with all-electronic measurement methods. More sensitive ways of measuring faradaic currents have therefore to be envisaged. An attractive method is to transform the faradaic current readout into a highly sensitive optical signal such as fluorescence.[7,8] Indeed, fluorescence-coupled electrochemical methodologies feature an intrinsic amplification mechanism since a one-electron transfer reaction can be related to a fluorescence event involving the emission of thousands of easily detectable photons. A basic prerequisite is obviously the technical ability to couple electron transfers to fluorescence generation. Such coupling is immediate when it comes to study electroactive species whose fluorescence is intrinsically modulated by their redox state.[9] Alternatively, when the species of interest is such that its electrochemical conversion generates local pH changes, a pH-sensitive fluorescent dye can be used as a reporter of the electron transfer process.[10–12] However, most species do not display these properties, nor can be endowed with them. Thus, it is appealing to develop new experimental schemes allowing electron transfer reactions of non-fluorescent (nor fluorogenic) molecules to be directly converted into independent fluorescence emission. So far, this has only been achieved in the unconventional "bipolar electrode" (BPE) configuration,[13–17] where an external driving voltage, applied through a non-wired conductive material, remotely polarizes the conductor in both anodic and cathodic poles, and thus electrically couples two spatially separated faradaic reactions. A "classical" (non-fluorogenic) redox reaction of interest occurs at one pole, while an electro-fluorogenic reaction is monitored at the other pole by optical microscopy. This design has been very recently scaled by Zhang et al. to nano-dimensions, in a bipolar nanoparticle scheme aiming at *optically* detecting single redox events by fluorescence measurements.[18]

However, the problem with bipolar electrochemistry is that the driving voltage applied to the BPE cell is, at best, only indirectly related to the thermodynamics of the faradaic electron transfer reaction of interest.[19,20] What is therefore needed is a way of coupling fluorescence emission with any electron transfer reaction *occurring at an electrode under potentiostatic control*, i.e. to which a thermodynamically relevant potential is directly applied. This is precisely what the instrumental scheme we introduce here is meant to achieve. Its working principle consists in coupling the electrochemical reaction of any species at the working electrode of a standard three electrode setup, with the production of a fluorescent species at the counter electrode. To establish the proof-of-concept of such a current-to-fluorescence conversion scheme, the oxidation of ferrocenedimethanol is coupled to fluorescence emission triggered by reduction of resazurin, a model electro-fluorogenic reaction.[14,21] The most effective experimental configuration enabling *conformal* transduction of the oxidative faradaic current into a fluorescence signal is identified, based on new quantitative mechanistic insights into resazurin electrochemistry, and electrode size (i.e. diffusion regime) considerations.

EXPERIMENTAL SECTION

Chemicals and solutions. Resazurin sodium salt, RZ (Bio-Reagent, dye content ~80%), resorufin, RF (dye content 95 %) and 1-1'-ferrocenedimethanol FcdiOH (97%) were Sigma-Aldrich products used as received. Aqueous 0.1 M carbonate buffer pH 10 was prepared with 60 mM sodium bicarbonate ($NaHCO_3$) and 40 mM sodium carbonate (Na_2CO_3) in double-deionized water (Milli-Q Millipore 18.2 MΩ cm^{-1} resistivity). A fresh RZ solution was daily prepared (in carbonate buffer) prior to use, and protected from light. All other chemicals were analytical grade products and used as received.

Electrochemical set-up coupled to epifluorescence microscopy. A standard three-electrode system was installed into a custom-made opto-electrochemical cell with one or two separated electrolytic compartments (~10 mL) according to the experimental configuration to consider (see Figure 1 for details). Both compartments have a flat clear window as the bottom, positioned in front of the objective of a wide-field microscope, to enable the visualization of the electrode surface of interest (working or counter electrode). Miniature Dri-Ref electrode (Dri-Ref-2SH, WPI) was used as electrode reference. All reported potentials are referenced vs. saturated calomel electrode (SCE) potential (+ 0.05 V vs. Dri-Ref).

Fluorescence imaging of electrode surfaces was performed using an inverted microscope (IX71, Olympus) interfaced with a potentiostat OGS100 (Origalys ElectroChem, France) controlled by its own software, for cyclic voltammetric (CV) measurement. The full equipment was placed in a Faraday cage. Light source was provided by a 100W halogen lamp through an epifluorescence mirror unit (U-MWG2, Olympus) adapted for the resorufin fluorophore: excitation light was selected through a 530 ± 20 nm bandpass filter, reflected at 90° by a 570 nm dichroic beamsplitter and focused on the electrode surface with a 10x0.25 NA objective (Olympus Plan 10X/0.25 Ph1). An additional 1.6x magnification was used for imaging ultramicroelectrodes. Fluorescence signal produced at the electrode was collected by the same objective, transmitted through the dichroic mirror and a 590 nm longpass emission filter, and finally directed onto a back-illuminated CMOS camera (KURO 1200B, Princeton Instruments, 95% QE, pixel size 11x11 μm). The electrode to image was immersed in the compartment containing the resazurin solution, and positioned in the focal plane of the objective with a micromanipulator (Sutter Instrument) under bright-field illumination. A distance of 500 μm between the electrode surface and the optical window was typically used. Fluorescence videos were then recorded, with a 100 ms exposure time per image, simultaneously with the cyclic voltammograms acquisitions at specified scan rates. Camera control and image processing were performed with the LightField 6.0 software (Princeton Instruments). Variation of fluorescence intensity over time was measured from a sequence of images of the same region of interest (ROI). For the 1 mm disk electrode, a large square ROI was chosen in the middle of the circular area of the electrode, where incident light appears uniformly distributed. For platinum ultramicroelectrode (UME) with 25 μm in diameter, a 100x100 pixels ROI (~70x70 μm in real scale) encompassing the electroactive area was used to collect fluorescence photons emitted by all resorufin molecules distributed in the whole expanding diffusion layer. Mean background intensity acquired on the very first image of each video was systematically subtracted from subsequent images to derive the voltfluorogram (CVF) profiles. Importantly, RZ and FcdiOH solu-

tions were degassed by bubbling argon for 20 minutes before experiments and between measurements. A blanket of argon was maintained above the solutions during the measurements.

Simulations. CVs and CVFs curves, at micro- and millimetric sized electrodes, were simulated using the DigiElch professional V7 and COMSOL Multiphysics 4.4 softwares respectively. All resazurin-type species were assumed to display the same diffusion coefficient as resorufin in aqueous medium (4.8 10^{-6} cm^2 s^{-1}).[22]

RESULTS AND DISCUSSION

The faradaic current to fluorescence emission conversion scheme we propose is presented in Figure 1A. It is based on a standard three electrode setup, using an opto-electrochemical cell with separated compartments. The solution containing the non-fluorescent species to be electrochemically addressed (e.g. to be oxidized) is placed in a first compartment, together with a working electrode and a reference electrode. The second compartment, connected to the first one via a classical porous glass-frit, contains a fluorogenic reporter species, e.g. introduced in its oxidized form. A counter electrode is placed in this compartment and its surface is imaged with an epifluorescence optical microscope. The three electrodes are connected to a classical potentiostat. This configuration allows to set the working electrode at any desired potential to trigger the oxidation of the species in the first compartment. The generated anodic current will necessarily be compensated by a cathodic current of *exactly* the same (absolute) intensity running through the counter electrode.
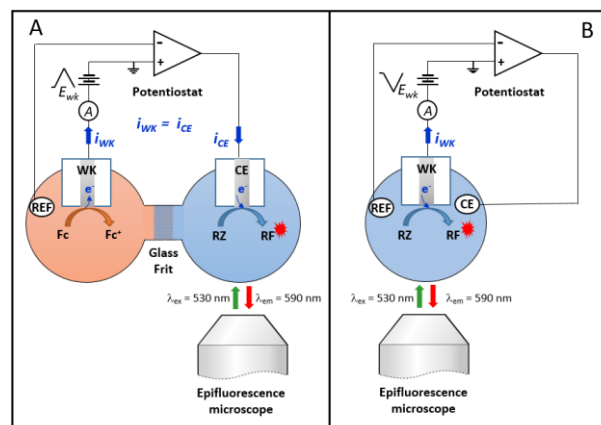
Figure 1. (A) Principle of the faradaic current-to-fluorescence converter setup proposed here. The electrochemical reaction at the working electrode (WK) is coupled, via the potentiostat, with the production of a fluorescent species at the counter electrode (CE). The faradaic current ($i_{WK} = i_{CE}$) is thus transduced into remote fluorescence emission. (B) Setup used for the mechanistic study of resazurin reduction by coupled cyclic voltammetry and voltfluorometry. Both current and fluorescence signals are recorded at the working electrode.

To generate such a current the potentiostat will automatically set the counter electrode potential so as to trigger the most immediately accessible reduction reaction delivering a sufficient amount of current. In proper conditions, this reaction will be the reduction of the fluorogenic dye introduced in the counter electrode compartment. As a result, electron transfers at the working electrode will become effectively detectable as a fluorescent signal at the counter electrode by the epifluorescence microscope.

The first conditions for achieving the current-to-fluorescence conversion, is to identify a suitable fluorogenic reporter molecule. For the present proof of concept experiments we chose the popular resazurin (RZ) dye.[14,21] Resazurin can be reduced irreversibly to resorufin (RF), in a complex process involving the transfer of 2 electrons, 2 protons and breaking of a N-O bond as depicted in Scheme 1. RF can be further reversibly reduced to dihydroresorufin (DH), via a 2 electron and proton transfer.[23,24]
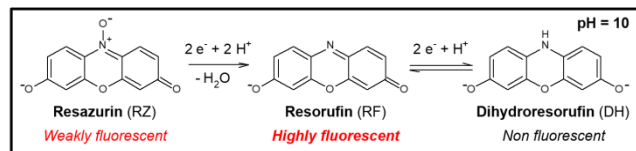
Scheme 1. Global scheme for the fluorogenic reduction of resazurin to resorufin, and then to dihydroresorufin, at pH 10.

Resazurin is the archetype of a species whose fluorescence is modulated by its redox state (and pH). Indeed the fluorescence of RZ, RF and DH differ markedly: RZ is only weakly fluorescent, RF is highly fluorescent, and DH is at the opposite non-fluorescent.[25,26] As a result RZ/DH electrochemistry has been used as the basis of a wealth of spectroelectrochemical systems aiming at coupling electron transfer events with fluorescence generation.[14,15,21,27]

Herein, we use the fluorogenic reduction of RZ to serve as a sensitive reporter of *oxidative* electron transfers. But, to achieve this goal, we first thought necessary to acquire more mechanistic insights into RZ reduction than currently available from literature. We therefore conducted cyclic voltammetry experiments, coupled with simultaneous fluorescence detection at the working electrode, as schematized in Figure 1B. For these, and all subsequent experiments, a 0.1 M carbonate buffer pH 10 was used as electrolyte, since these conditions were previously used in literature to study the electro-fluorochromic properties of resazurin and resorufin.[21,28] Besides, at such basic pH, the fluorescence emission intensity of these dyes is maximal.[25]

Transient cyclic voltammetry and voltfluorometry of resazurin. Cyclic voltammograms (CVs, current intensity, i, vs. electrode potential, E) and cyclic voltfluorograms (CVFs, fluorescence intensity vs. E) of resazurin were simultaneously acquired. Typical CV and CVF signals, recorded at a 1 mm disk electrode, are respectively shown in Figure 2A and Figure 2B. The electrode potential was scanned form -0.15 to -0.75 V/SCE at a scan rate $v = 0.1$ V s^{-1}. The CV displays two cathodic peaks, located respectively around -0.49 V/SCE and -0.62 V/SCE, and a less intense anodic peak around -0.42 V/SCE. As reported in literature the first cathodic peak is assigned to the reduction of RZ into RF, the second to the reduction of RF into DH, and the anodic peak assigned to the back-oxidation of DH into RF.[14,21,23,24].
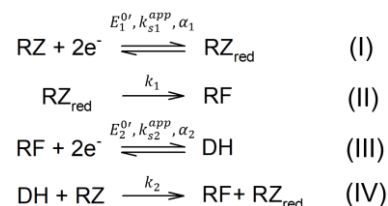
Examining the CVF signal reproduced in Figure 2B, one sees that the onset of fluorescence occurs around $E \sim$ -0.4 V/SCE, which is concomitant with the beginning of the electrochemical reduction of RZ into the highly fluorescent RF species. As the electrode is scanned more cathodically, the fluorescence signal is observed to increase continuously, even in potential regions where RF is consumed at the electrode and converted into the non-fluorescent species DH. This apparent discrepancy actually evidences the occurrence of a comproportionation reaction according to which the highly reduced DH species

reduces RZ into RF. As a result the fluorescent species RF is de facto produced all along the potential scan. Occurrence of this reaction for RZ reduction has been recently evidenced by confocal fluorescence microscopy studies.
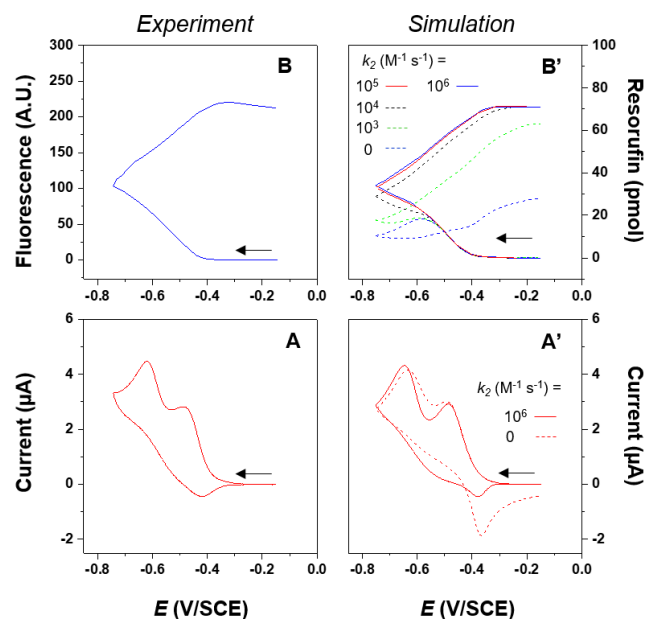
Figure 2. (A) Experimental cyclic voltammogram (CV) of 1 mM resazurin at a 1 mm diameter platinum working electrode, and (B) simultaneously recorded voltfluorogram (CVF). 0.1 M carbonate buffer pH 10, scan rate 0.1 V s^{-1}. (A') Simulated CVs and (B') simulated molar amount of resorufin in the diffusion layer (N_{RF}) vs. the electrode potential, E, calculated using DigiElch for various values of the comproportionation rate constants k_2, as indicated.

In order to get quantitative insights into the relation between current and fluorescence generation, we propose the following simple mechanism to describe the reactions associated with resazurin reduction at the electrode (at pH = 10), scheme 2.

$$RZ + 2e^- \underset{}{\overset{E_1^{0\prime}, k_{s1}^{app}, \alpha_1}{\rightleftharpoons}} RZ_{red} \qquad (I)$$

$$RZ_{red} \xrightarrow{k_1} RF \qquad (II)$$

$$RF + 2e^- \underset{}{\overset{E_2^{0\prime}, k_{s2}^{app}, \alpha_2}{\rightleftharpoons}} DH \qquad (III)$$

$$DH + RZ \xrightarrow{k_2} RF + RZ_{red} \qquad (IV)$$

Scheme 2. Formal mechanism for the electroreduction of resazurin, and of the thus produced resorufin.

RZ reduction at the electrode is modeled as a direct two-electron reduction transfer reaction, characterized by an apparent standard potential $E_1^{0\prime}$, a heterogeneous electron transfer rate constant k_{s1}^{app} and a charge transfer coefficient α_1, reaction (I). A chemical step, characterized by a first order rate constant k_1, and corresponding to the breaking of the N-O bound of the intermediate species RZ$_{red}$ (formal "reduced resazurin" species) is then assumed to produce RF, reaction (II). Admittedly, RZ reduction at the electrode and RF production may actually rather follow a fully concerted pathway,[29] but the assumption of a sequential process is, as shown below, sufficient to account for the experimental data collected here. Resorufin reduction, occurring at the level of the second CV wave, is also modeled as

the direct transfer of two electrons characterized by the set of apparent parameters $E_2^{0\prime}$, k_{s2}^{app}, α_2, reaction (III). This is a deliberate simplification, as the successive transfer of 2 electrons and protons may only be accurately described by a direct 2 electron transfer in limiting kinetic situations.[30–33] Yet, in the absence of extensive data regarding the actual reduction mechanism of RF this simplification is required. Finally, the thermodynamically favorable homogeneous comproportionation reaction between DH and RZ,[28] yielding RF and RZ$_{red}$, is represented by reaction (IV), and characterized by the second order rate constant k_2.

We now intend to make use of the proposed mechanism to simulate the experimental CV and CVF of resazurin we recorded, using the DigiElch software. This simulation requires that all of the parameters appearing in the above kinetic scheme are quantitatively known, or that further simplifying assumptions are made. The most easily accessible parameters are those related to the reduction of resorufin, as its CV response can be recorded in separate experiments. Analysis of the CV of RF, carried out as detailed in Supporting Information, Section-1, actually allows to derive the following values: $E_2^{0\prime} = -0.465$ V/SCE, $k_{s2}^{app} = 6.8 \ 10^{-5}$ cm s^{-1}, $\alpha_2 = 0.35$. The low value obtained for k_{s2}^{app}, and a α_2 value significantly differing from 0.5, are both typical of sequential e$^-$/H$^+$ electron transfer reactions at an electrode.[30–33] Indeed, because of the rapid protonation of the species produced by the individual electron transfer steps, e$^-$/H$^+$ reactions in water are typically characterized by very slow apparent electron transfer rate constants.[33] This also conceptually applies to the direct 2e$^-$ reduction of RZ to RZ$_{red}$, reaction (I), which can thus be safely regarded as being slow with respect to the subsequent bond-breaking reaction (II). In this situation, kinetic control is by the electron transfer reaction and no information regarding the value of k_1 can be obtained from CV analysis.[34]

The first RZ reduction wave then simply corresponds to an irreversible 2 electron transfer signal, from which only the parameter α_1 can be immediately derived. By measuring the half-width of the wave, theoretically given by $29.6/2\alpha_1$, we find $\alpha_1 = 0.39$. We note that this value is close to the one derived for α_2. The only parameters still undetermined at this stage are now $E_1^{0\prime}$, k_{s1}^{app} and k_2. Considering the similar nature of the e$^-$/H$^+$ transfer reactions (I) and (III), it seems reasonable to assume that the values of k_{s2}^{app} and k_{s1}^{app} are of the same order of magnitude. For simplicity we decided to set $k_{s1}^{app} = k_{s2}^{app}$. We then verified that, as expected, with such a low k_{s1}^{app} value, simulated CVs did not depend on the value assigned to k_1, down to unrealistically low values of ~5 s^{-1} (see SI, Section-2).

We were then able to run simulations using the sole values of k_2 and of $E_1^{0\prime}$ as adjustable parameters, trying to reproduce the experimental signal shown in Figure 2A. In doing so we observed that the first reduction wave of the simulated CV was insensitive to the value set for k_2. This can be seen in Figure 2A' where voltammograms simulated for extreme values of k_2 ($k_2 = 0$, dashed curve, and $k_2 = 10^6$ M^{-1} s^{-1}, solid curve) are compared. This result falls in line with the well-documented fact that, in the simpler case of two stepwise one electron transfer reactions (EE schemes), comproportionation reactions have little or no effect on the voltammetry signals.[35–37] The second cathodic wave also showed little dependence on k_2 values. As a result, accurate k_2 values cannot be obtained by analyzing the cathodic waves of the experimental CV signal. At the opposite, the peak potential of the first wave showed a marked dependence on the value set for $E_1^{0\prime}$. This allowed us to derive a single parameter best fit value of $E_1^{0\prime} = -0.33$ V/SCE.

In order to derive the missing k_2 value, we turned to the analysis of the CVF signal. Indeed, unlike the current signal, the fluorescence signal is expected to be strongly dependent on the rate of comproportionation, since this reaction ultimately generates two RF molecules from the non or weakly fluorescent DH and RZ species. In order to assess this dependence theoretically, the molar amount of RF species present in the diffusion layer, N_{RF}, was derived from simulation, for any electrode potential E, and for various k_2 values. The thus obtained N_{RF} vs. E curves, shown in Figure 2B', can be considered as equivalents to voltfluorograms. One can see that on the cathodic potential scan, N_{RF} (hence the fluorescence signal) is expected to increase at the level of the first cathodic wave, no matter the k_2 value. But it is also observed that, in the absence of comproportionation ($k_2 = 0$), N_{RF} decreases in the potential region corresponding to the second CV wave, i.e. when RF is consumed to produce DH. Some fluorescence intensity is recovered in the anodic trace due to the oxidation of DH to RF at the electrode.

The mere fact that no such fluorescence decay was observed in our experimental CVFs is an indication that comproportionation reaction (IV) actually takes place at a significant rate. Indeed, it appears from Figure 2B' that an ever increasing fluorescence signal, as was experimentally observed, implies a k_2 value in excess of 10^4 M^{-1} s^{-1}. Actually, reproducing closely the shape of the experimental CVF required to set a minimal value of $k_2 \sim 10^5$ M^{-1} s^{-1} (compare Figure 2B and Figure 2B'). Deriving a more accurate value for k_2 is difficult since the shape of the simulated N_{RF} vs. E variation was observed to change little when k_2 was increased above 10^5 M^{-1} s^{-1}. This value sets a lower bound for the actual rate constant of the comproportionation reaction between DH and RZ. We also verified that, by setting k_2 values in excess of 10^5 M^{-1} s^{-1} a good match between experimental and theoretical CVs could be obtained (compare Figure 2A and Figure 2A'). These later results actually demonstrates that the comproportionation reaction (IV) can legitimately be considered as being infinitely fast, as had been so far simply hypothesized in literature.[28] Overall, current generation and fluorescence emission are kinetically controlled by the electron transfer reactions of RZ and RF at the electrode.

Hence, at this stage of our work, analysis of the CV and CVF signals of RZ recorded simultaneously at a millimetric electrode allowed us to propose a simple mechanism, and to derive the values of the thermodynamic and kinetic constants required for reproducing the experimental CV and CVF signals quantitatively.

Yet, the above results also illustrated that, as can be seen by comparing Figure 2A and Figure 2B, the fluorescence and the electrochemical signals recorded at a millimetric electrode do not match in shape at all, nor adequately do the derivative of the fluorescence signal and the current (see Supporting Information). The reason for this shape mismatch is rooted to the fact that mass transport at millimetric electrodes is controlled by planar transient diffusion, which results in RF accumulation in the vicinity of the electrode. Therefore, it can be concluded that electrochemistry of a fluorogenic species at a millimetric electrode cannot be the basis of the current-to-fluorescence conversion system we aim to develop here, where fluorescence detection has to closely follow the current signal. We therefore turned to voltammetry at an ultramicroelectrode.

Stationnary cyclic voltammetry and voltfluorometry of resazurin at an ultramicroelectrode. The cyclic voltammogram and voltfluorogram of resazurin simultaneously recorded at a 25 μm diameter platinum ultramicroelectrode (UME) are presented in Figure 3. The experimental CV signal (Figure 3A) displays two successive S-shaped cathodic waves. The first is ascribable to the reduction of RZ into RF and the second of RF into DH. Most interestingly, one notices that the CVF signal, shown in Figure 3B, also displays two S-shaped waves closely corresponding in shape and in potential to the CV waves. Actually such a correspondence can be better apprehended by plotting the fluorescence signal as a function of the simultaneously recorded current, as shown in Figure 4A.
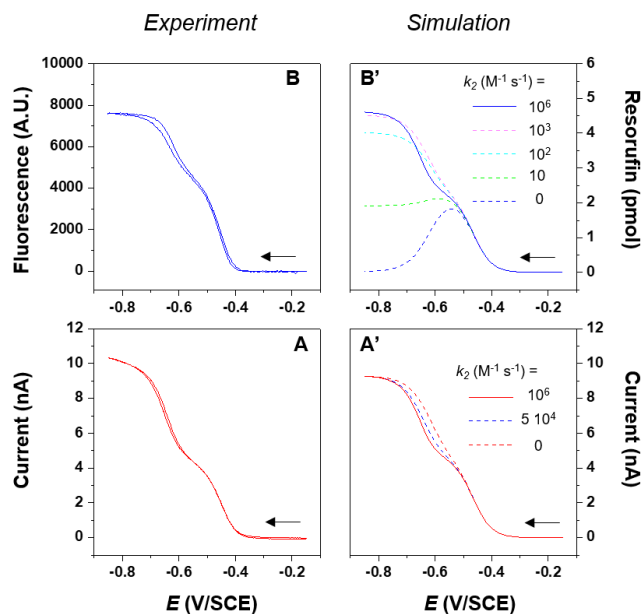
Figure 3. (A) Experimental CV of 1 mM resazurin at a 25 μm diameter platinum UME and (B) simultaneously recorded voltfluorogram CVF. 0.1 M carbonate buffer pH 10, scan rate 0.01 V s^{-1}. (A') Stationary theoretical CV and (B') molar amount of resorufin (N_{RF}) in the electrode vicinity vs. E, calculated using COMSOL for various values of the comproportionation rate constant k_2, as indicated.
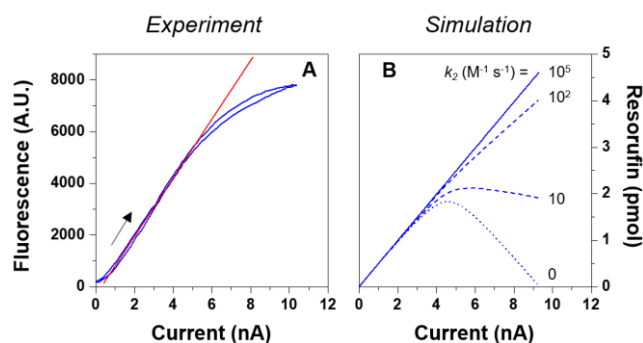

Figure 4. (A) Fluorescence intensity recorded at a 25 μm platinum UME where reduction of resazurin takes place, as a function of the UME current, i (corresponding CVs and CVFs are presented in Figure 3). (B) Simulated dependence of the molar amount of resorufin (N_{RF}) in the electrode vicinity as a function of the UME current, calculated for various values of the comproportionation rate constant k_2 as indicated.

One can then observe that the fluorescence signal is actually almost exactly proportional to the current signal, at least up to

current values around ~6 nA. Referring to Figure 3A it appears that this linear behavior corresponds to electrode potential regions encompassing the first cathodic wave, and extending well-into the second reduction CV wave. Deviation from linearity of the fluorescence vs. current plot for higher current values may be explained by the fact that, in the corresponding very cathodic potential region, some background current, not ascribable to RZ electrochemistry is detected. This is evidenced by the sloppy plateau displayed by the CV in the -0.75 to -0.8 V/SCE region, Figure 3A (also see Figure S1).

We then turned to simulation in an attempt to reproduce theoretically the electrochemical behavior and associated fluorescence emission recorded at the UME. For this we implemented under COMSOL the RZ reduction mechanism derived above, and calculated both the theoretical stationary voltammograms at a 25 μm electrode, and also the total quantity of resorufin, N_{RF}, present in the vicinity of the electrode (within a hemispherical domain 250 μm in radius extending away from the electrode surface). Simulations were first carried out with the set of kinetic parameters derived from the above transient cyclic voltammetry and voltfluorometry mechanistic investigations. This allowed us to very satisfyingly reproduce both the experimental CV and CVF signals recorded at the UME, without any adjustable parameters (Figure 3). This result further validated our kinetic model for RZ reduction.

We also used COMSOL simulations to investigate theoretically how the current and fluorescence signals (and their correlation) depended on the rate of the comproportionation reaction, which is key to sustained generation of fluorescence. We therefore calculated theoretical CVs and CVFs for various values of the comproportionation rate constant k_2. One can observe in Figure 3A' that the first reduction wave of the simulated CVs, is, as expected, largely insensitive to the rate of comproportionation. Considering now the simulated CVF, Figure 3B', one sees that, in the absence of comproportionation ($k_2 = 0$) a total extinction of fluorescence is expected to occur at the level of the second cathodic wave (RF to DH reduction). Yet, it also appears that the advent of even a slow comproportionation reaction ($k_2 = 10$ M^{-1} s^{-1}) is sufficient for fluorescence not to extinguish during the potential scan. Actually a value of $k_2 = 100$ s^{-1} is sufficient to bring the fluorescence intensity close to the maximum value it can reach for very fast comproportionation reaction ($k_2 \geq 10^5$ M^{-1} s^{-1}). These data finally allowed us to construct simulated current vs. fluorescent plots for various k_2 values. As evidenced in Figure 4B, in the range of current corresponding to the first reduction wave (below 4 nA here), proportionality between the current and the amount of RF present in the vicinity of the electrode (i.e. the fluorescence intensity) is predicted to be always verified, independently from the comproportionation reaction rate. For higher currents, i.e. in the potential region where RF reduction occurs ($i > 4$ nA), this linear behavior is verified only provided that $k_2 > 100$ M^{-1} s^{-1}. Such a condition is obviously met here, since we determined above that $k_2 > 10^5$ M^{-1} s^{-1}.
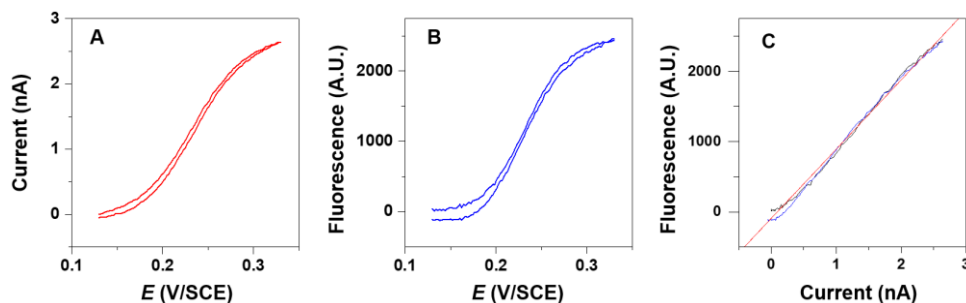
Figure 5. Converting a faradaic current into a fluorescence signal. The oxidation of ferrocenedimethanol (FcdiOH) at an electrode under potentiostatic control, was coupled to fluorescence emission arising from resazurin reduction, using the converter setup described in Figure 1A. (A) Cyclic voltammogram of FcdiOH at a 25 µm glassy carbon working ultramicroelectrode. (B) Fluorescence signal simultaneously recorded at a 25 µm diameter platinum counter ultramicroelectrode. (C) Intensity of the fluorescence signal versus the working electrode current. The working and counter electrode compartments contained respectively 1 mM FcdiOH in a 0.1 M NaClO$_4$ aqueous solution, and 0.5 mM resazurin in 0.1 M carbonate buffer pH 10. Scan rate 0.01 V s^{-1}.

Therefore, we have theoretically substantiated our unprecedented experimental observation that fluorescence generated at an ultramicroelectrode where reduction of RZ occurs is proportional to the current. This proportionality is obviously a benefit of the stationary spherical diffusion regime at UMEs that prevents accumulation of the electrogenerated RF species in the vicinity of the electrode surface. In literature, it has been shown that such an accumulation could also be avoided by introducing in solution a species which chemically scavenges RF (glucose in a 0.5 M NaOH medium), likewise this resulted in direct correlation between current and fluorescence.[15] We show here that simple spherical diffusion at an UME is actually enough to yield *close to perfect proportionality* between current and fluorescence in a much simpler and milder way.

We thus have identified an appropriate configuration where fluorescence can be used as a reliable reporter for the electrochemical current, an indispensable prerequisite for developing a current-to-fluorescence converter setup.

Converting a faradaic current generated at an electrode under potentiostatic control into fluorescence emission – proof of principle. As explained above the idea behind the setup we propose, represented in Figure 1A, is that, by virtue of the three electrode configuration, any electrochemical reaction is bound to be coupled with a counter-reaction at the counter electrode. The above work suggests that provided we make sure that this counter reaction is RZ reduction, and that the counter electrode is an UME, the fluorescence intensity should closely track the current generated at the working electrode. In order to establish the proof of concept of this original yet simple coupling scheme, we made use of an electrochemical cell comprising two separated compartments as shown in Figure 1A. Ferrocenedimethanol (FcdiOH) was introduced in the working electrode compartment and resazurin in the counter electrode compartment. The working electrode was a 25 µm diameter glassy carbon electrode, and the counter electrode a platinum electrode similar in size. The epifluorescence microscope was focused on the *counter electrode* surface.

The potential of the working electrode was scanned anodically at 0.01 V s^{-1}, in order to trigger FcdiOH oxidation, and back. The working electrode current was recorded simultaneously with the fluorescence emission at the counter electrode. When plotting the working electrode current as a function of its potential *E,* the expected S-shaped voltammogram, typical of FcdiOH electrochemistry at a microelectrode, was obtained

(Figure 5A).[38] Remarkably, the voltfluorogram obtained by plotting the fluorescence intensity recorded *at the counter electrode* versus *E,* was very similar in shape to the voltammogram recorded at the working electrode (Figure 5B). Actually, the similarity between these two signals can be better assessed by plotting the fluorescence intensity recorded at the counter electrode as a function of the current recorded at the working electrode. One can see from Figure 5C that the obtained plot is almost perfectly linear. This shows that we have achieved the sought configuration, where fluorescence emission at the counter electrode perfectly tracks the working electrode current.

Herein, on the basis of the model FcdiOH/RZ system, we thus have demonstrated how an electrochemical reaction of a non-fluorescent (nor fluorogenic) species at an electrode *under potentiostatic control* can be quantitatively coupled to fluorescence emission. Our new coupling scheme, by effectively converting faradaic electron transfers into fluorescence emission, opens avenues for achieving amplification of low intensity electrochemical signals via highly sensitive optical probing. Some important characteristics, and foreseeable limits/advantages, of this new experimental approach are discussed below.

The setup we designed here has first to be made more versatile in order to enable the measurement of both anodic and also cathodic currents. This requires identifying an oxidizable fluorogenic species amongst those already reported in literature, to be added to the counter electrode compartment together with RZ. Amplex-red, a molecule whose oxidation at an electrode was shown to yield resorufin,[39,40] would be a very good candidate.

The limit in sensitivity of our current-to-fluorescence converter setup will also have to be explored. The current to be transduced into a fluorescence signal has to be such that the counter electrode is kept at a potential in the -0.4 to -0.6 V/SCE region, where current and fluorescent intensity are ideally proportional. This requires matching the radius of the counter electrode UME, a_{CE}, and the resazurin concentration, C_{RZ}, so that the intensity of the current to be measured is such that: $i \leq 8FDa_{CE}C_{RZ}$, with D the diffusion coefficient of the fluorogenic species. This condition sets a maximum limit to the current that can be transduced (measured) by fluorescence emission with a given set of a_{CE} and C_{RZ} values. This constrain is actually reminiscent of adjusting the "gain" of an ammeter as a function of the maximum current intensity to be measured.

The lowest current intensity measurable is expected to be in part limited by the emitted-photons collection efficiency and the sensibility of the camera. The optical limit-of-detection issue of this platform could be investigated by designing an optimized epifluorescence scheme allowing to reduce the background (out-of-focus) light and the inner-filter effects inherent to such a wide-field microscopy. Yet one should also note that measuring lower currents will require using smaller counter electrode UMEs and/or lower RZ concentration in order for the potentiostat to bias the counter electrode at a potential negative to the onset of RZ reduction, i.e. past -0.4 V/SCE.

The bandwidth of the setup (reciprocal of its response time) is dictated by the requirement of keeping mass transport at the counter electrode UME in the stationary diffusion regime. The response time corresponds to the time, t, it takes for RF to leave the stationary diffusion layer developing around the counter electrode UME. It is given coarsely by $t = a_{CE}^{2}/D$. Consequently, the size of the counter electrode UME has to be adapted to the desired bandwidth. This bandwidth will depend on the "gain", via the a_{CE} value, in the exact opposite way it does for an ammeter: high bandwidth and low current measurement will not be mutually exclusive, but at the opposite will be both achievable with small diameter counter ultramicroelectrodes.

CONCLUSION

First, we have examined, by coupled cyclic voltammetry and voltfluorometry, the reduction of resazurin at a millimetric electrode, and the concomitant fluorescence emission. We proposed a workable kinetic model allowing to quantitatively account for the experimental electrochemical current and fluorescence signals. The role of the comproportionation reaction on the current and fluorescence generation was notably deciphered. Overall, we showed that fluorescence emission is kinetically controlled by the (slow) electron transfer reactions of resazurin and resorufin at the electrode. Kinetic and thermodynamic parameters describing these reactions were determined.

Second, we demonstrated experimentally, and substantiated by simulation, that, provided the working electrode is an ultramicroelectrode, the fluorescence and current signals generated by resazurin reduction are rigorously proportional to each other. This so far unreported property of resazurin electrochemistry is a clear benefit of the spherical diffusion regime that can be experimentally achieved at small enough ultramicroelectrodes.

Third, by exploiting this unique property, and the built-in ability of potentiostats to couple redox reactions, we demonstrated that an oxidation reaction occurring at a working electrode can be coupled to resazurin reduction at an (ultramicro)counter electrode, so that the generated current is transduced into conformal fluorescence emission.

This is the first demonstration that electron transfer of a non-fluorescent (nor fluorogenic) species at an electrode under potentiostatic control can be transformed in a remote quantified fluorescence signal. We believe that, due to the extreme sensibility of fluorescence detection, this original coupling scheme may ultimately enable detecting *optically* individual electron transfer events (or extremely low faradaic currents) that cannot be directly measured electronically.

ASSOCIATED CONTENT

Supporting Information

AUTHOR INFORMATION

Corresponding Author

* E-mail: christophe.demaille@univ-paris-diderot.fr
* E-mail: arnaud.chovin@univ-paris-diderot.fr

Notes

The authors declare no competing financial interest

ACKNOWLEDGMENT

REFERENCES

(1)   Zevenbergen, M. A. G.; Singh, P. S.; Goluch, E. D.; Wolfrum, B. L.; Lemay, S. G. *Nano Lett.* **2011**, *11*, 2881–2886.

(2)   Kang, S.; Nieuwenhuis, A. F.; Mathwig, K.; Mampallil, D.; Lemay, S. G. *ACS Nano* **2013**, *7*, 10931–10937.

(3)   Fan, F.-R. F.; Kwak, J.; Bard, A. J. *J. Am. Chem. Soc.* **1996**, *118*, 9669–9675.

(4)   Byers, J. C.; Paulose Nadappuram, B.; Perry, D.; McKelvey, K.; Colburn, A. W.; Unwin, P. R. *Anal. Chem.* **2015**, *87*, 10450–10456.

(5)   Nault, L.; Taofifenua, C.; Anne, A.; Chovin, A.; Demaille, C.; Besong-Ndika, J.; Cardinale, D.; Carette, N.; Michon, T.; Walter, J. *ACS Nano* **2015**, *9*, 4911–4924.

(6)   Chennit, K.; Trasobares, J.; Anne, A.; Cambril, E.; Chovin, A.; Clément, N.; Demaille, C. *Anal. Chem.* **2017**, *89*, 11061–11069.

(7)   Mathwig, K.; Aartsma, T. J.; Canters, G. W.; Lemay, S. G. *Annu. Rev. Anal. Chem.* **2014**, *7*, 383–404.

(8)   Fan, Y.; Anderson, T. J.; Zhang, B. *Curr. Opin. Electrochem.* **2018**, *7*, 81–86.

(9)   Bouffier, L.; Doneux, T. *Curr. Opin. Electrochem.* **2017**, *6*, 31–37.

(10)   Engstrom, R. C.; Ghaffari, S.; Qu, H. *Anal. Chem.* **1992**, *64*, 2525–2529.

(11)   Cannan, S.; Macklam, I. D.; Unwin, P. R. *Electrochem. commun.* **2002**, *4*, 886–892.

(12)   Yang, M.; Batchelor-McAuley, C.; Kätelhön, E.; Compton, R. G. *Anal. Chem.* **2017**, *89*, 6870–6877.

(13)   Fosdick, S. E.; Knust, K. N.; Scida, K.; Crooks, R. M. *Angew. Chemie Int. Ed.* **2013**, *52*, 10438–10456.

(14)   Guerrette, J. P.; Percival, S. J.; Zhang, B. *J. Am. Chem. Soc.* **2013**, *135*, 855–861.

(15)   Oja, S. M.; Guerrette, J. P.; David, M. R.; Zhang, B. *Anal. Chem.* **2014**, *86*, 6040–6048.

(16)   Xu, W.; Ma, C.; Bohn, P. W. *ChemElectroChem* **2016**, *3*, 422–428.

(17)   Bouffier, L.; Doneux, T.; Goudeau, B.; Kuhn, A. *Anal. Chem.* **2014**, *86*, 3708–3711.

(18)   Fan, Y.; Hao, R.; Han, C.; Zhang, B. *Anal. Chem.* **2018**, *90*, 13837–13841.

(19)   Guerrette, J. P.; Oja, S. M.; Zhang, B. *Anal. Chem.* **2012**, *84*, 1609–1616.

(20)   Cox, J. T.; Guerrette, J. P.; Zhang, B. *Anal. Chem.* **2012**, *84*,

8797–8804.

(21) Doneux, T.; Bouffier, L.; Goudeau, B.; Arbault, S. *Anal. Chem.* **2016**, *88*, 6292–6300.

(22) Schilling, E. A.; Kamholz, A. E.; Yager, P. *Anal. Chem.* **2002**, *74*, 1798–1804.

(23) Twigg, R. S. *Nature* **1945**, *155*, 401–402.

(24) Khazalpour, S.; Nematollahi, D. *RSC Adv.* **2014**, *4*, 8431–8438.

(25) Bueno, C.; Villegas, M. L.; Bertolotti, S. G.; Previtali, C. M.; Neumann, M. G.; Encinas, M. V. *Photochem. Photobiol.* **2002**, *76*, 385–390.

(26) Porcal, G. V; Previtali, C. M.; Bertolotti, S. G. *Dye. Pigment.* **2009**, *80*, 206–211.

(27) Oja, S. M.; Zhang, B. *Anal. Chem.* **2014**, *86*, 12299–12307.

(28) de Poulpiquet, A.; Goudeau, B.; Garrigue, P.; Sojic, N.; Arbault, S.; Doneux, T.; Bouffier, L. *Chem. Sci.* **2018**, *9*, 6622–6628.

(29) Costentin, C. *Chem. Rev.* **2008**, *108*, 2145–2179.

(30) Laviron, E. *J. Electroanal. Chem.* **1983**, *146*, 1–13.

(31) Laviron, E. *J. Electroanal. Chem.* **1983**, *146*, 15–36.

(32) Laviron, E. *J. Electroanal. Chem.* **1984**, *164*, 213–227.

(33) Marchal, D.; Boireau, W.; Laval, J. M.; Bourdillon, C.; Moiroux, J. *J. Electroanal. Chem.* **1998**, *451*, 139–144.

(34) Nadjo, L.; Savéant, J. M. *J. Electroanal. Chem.* **1973**, *48*, 113–145.

(35) Lehmann, M. W.; Evans, D. H. *Anal. Chem.* **1999**, *71*, 1947–1950.

(36) Amatore, C.; Bonhomme, F.; Bruneel, J.-L.; Servant, L.; Thouin, L. *J. Electroanal. Chem.* **2000**, *484*, 1–17.

(37) Klymenko, O. V; Svir, I.; Amatore, C. *Electrochem. Commun.* **2010**, *12*, 1378–1382.

(38) Zevenbergen, M. A. G.; Wolfrum, B. L.; Goluch, E. D.; Singh, P. S.; Lemay, S. G. *J. Am. Chem. Soc.* **2009**, *131*, 11471–11477.

(39) Lefrançois, P.; Vajrala, V. S. R.; Arredondo, I. B.; Goudeau, B.; Doneux, T.; Bouffier, L.; Arbault, S. *Phys. Chem. Chem. Phys.* **2016**, *18*, 25817–25822.

(40) Malytska, I.; Doneux, T.; Bougouma, M.; Kuhn, A.; Bouffier, L. *J. Phys. Chem. C* **2019**, *123*, 5647–5652.

for TOC only